

Supplementary Material for:

Late complex tensile fracturing interact with topography at Cumbre Vieja, La Palma

T. R. Walter^{*α}, E. Zorn^α, P.J. Gonzalez^β, E. Sansosti^χ, V. Munoz^α, A.V. Shevchenko^α, S. Plank^δ, D. Reale^χ, N. Richter^{α, ε}

^α GFZ German Research Centre for Geosciences, Telegrafenberg, 14473 Potsdam, Germany

^β Department of Life and Earth Sciences, Instituto de Productos Naturales y Agrobiología, Consejo Superior de Investigaciones Científicas (IPNA-CSIC). Avda. Astrofísico Francisco Sanchez, 3, 38206, La Laguna, Tenerife, Spain.

^χ National Research Council (CNR), Institute for Electromagnetic Sensing of Environment (IREA), via Diocleziano 328, 80124 Napoli, Italy

^δ German Aerospace Center (DLR), German Remote Sensing Data Center, 82234 Oberpfaffenhofen, Germany

^ε now at: Remote sensing of natural hazards, RWTH Aachen University, Lochnerstr. 4-20, 52056 Aachen, Germany

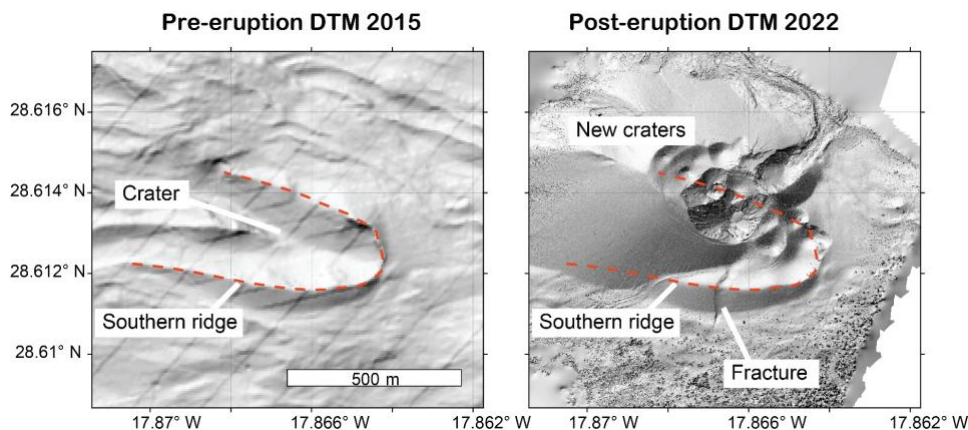


Figure S1

Comparison of hill shade topography maps before and after the eruption. The data before the eruption is MDT02, a 2-m resolution LiDAR dataset acquired in 2015 and freely available at CNIG (MDT02-ETRS89-HU28-1085-2-COB2, link provided below). The data after the eruption is our own data acquired by RTK drone on 15 Jan 2022. The red dashed line is the trace of the open crater rim in the 2015 dataset, still visible in the 2022 dataset.

<https://centrodedescargas.cnig.es/CentroDescargas/buscador.do?palma=S>

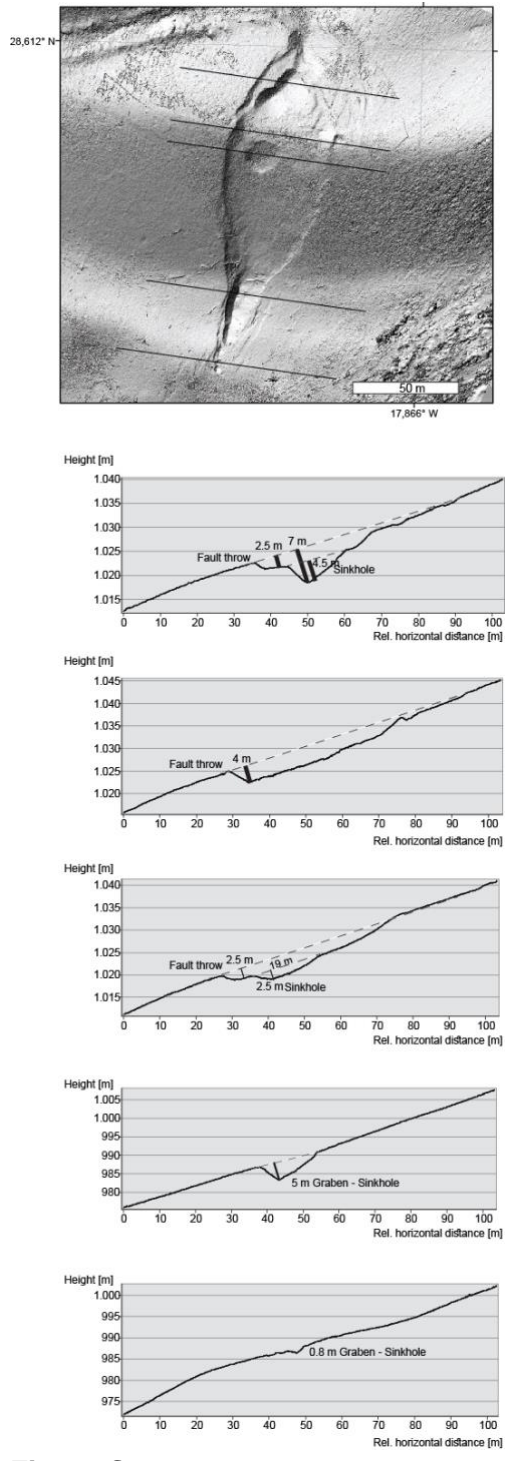


Figure S2

Hillshade topography map showing the fracture on 5 December 2021, and profiles across, from north to south. Maximum vertical throw of the fault is 4 m, decreasing to <1 m at the northern and southern edges, higher values are found at higher parts of the topographic ridge and where colocated sinkholes can be identified. Note that some sinkholes have 4.5 m vertical throw and up to ~20 m diameter.

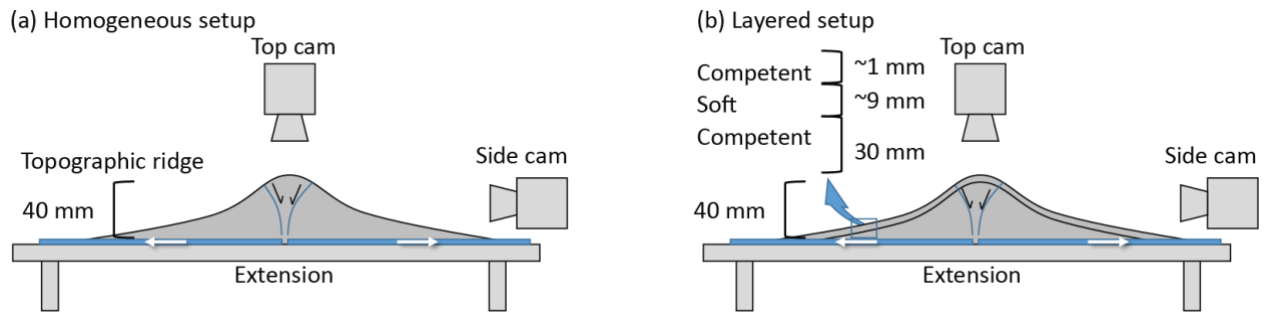
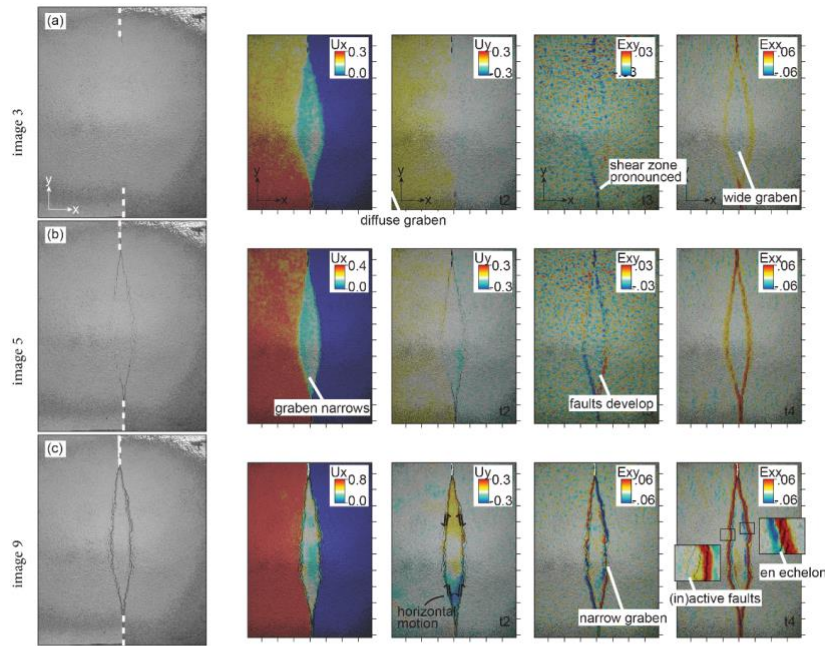


Figure S3

Setup of experiments, left in a homogeneous setup, right in a similar setup with a 10 mm layer of soft (low cohesive) pure sand on it.

Homogeneous experiments



Heterogeneous experiments

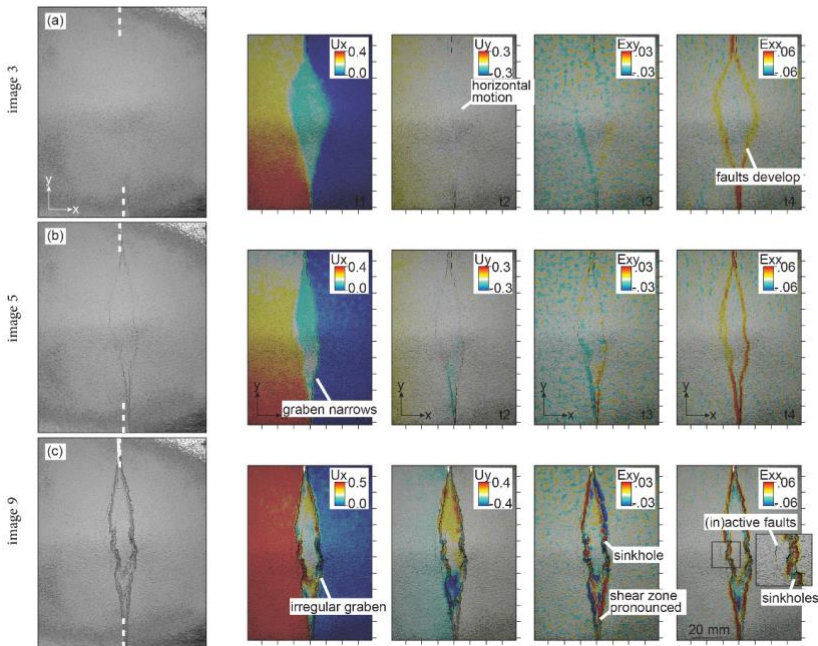
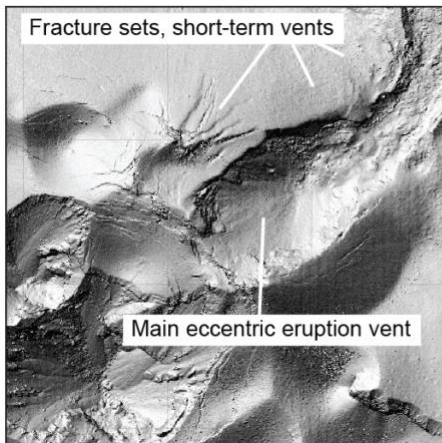


Figure S4

Experimental results for homogeneous setup (top) and heterogeneous setup (bottom). The fault complexity, deviation and step over increase in the heterogeneous setup, where also the number and dimension of sinkholes increase visibly. Sinkholes in such a layered (heterogeneous) media have been already studied {Ferrill, 2004 #3497;Hardy, 2021 #3498}.

(a) Shaded relief of northern vent



(b) Camera recording of multiple vents

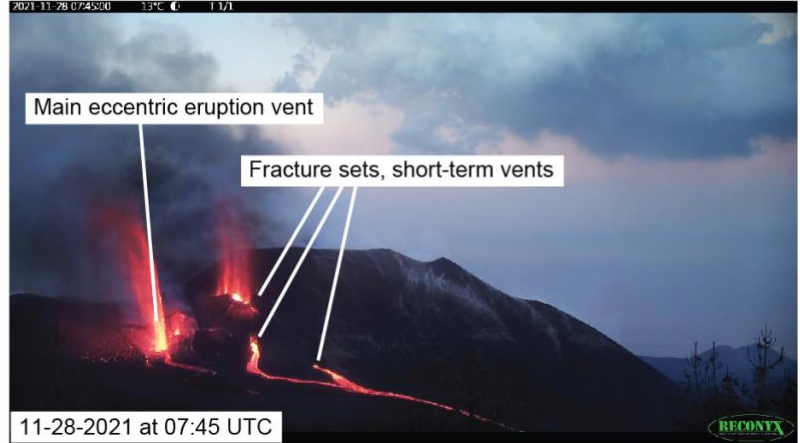


Figure S5

Fracture sets develop to the north of the eccentric northern eruption, indicating temporary extension of the fracture. Tephra deposition covered these vents later again, but their presence is depicted in the camera data shown in (b).

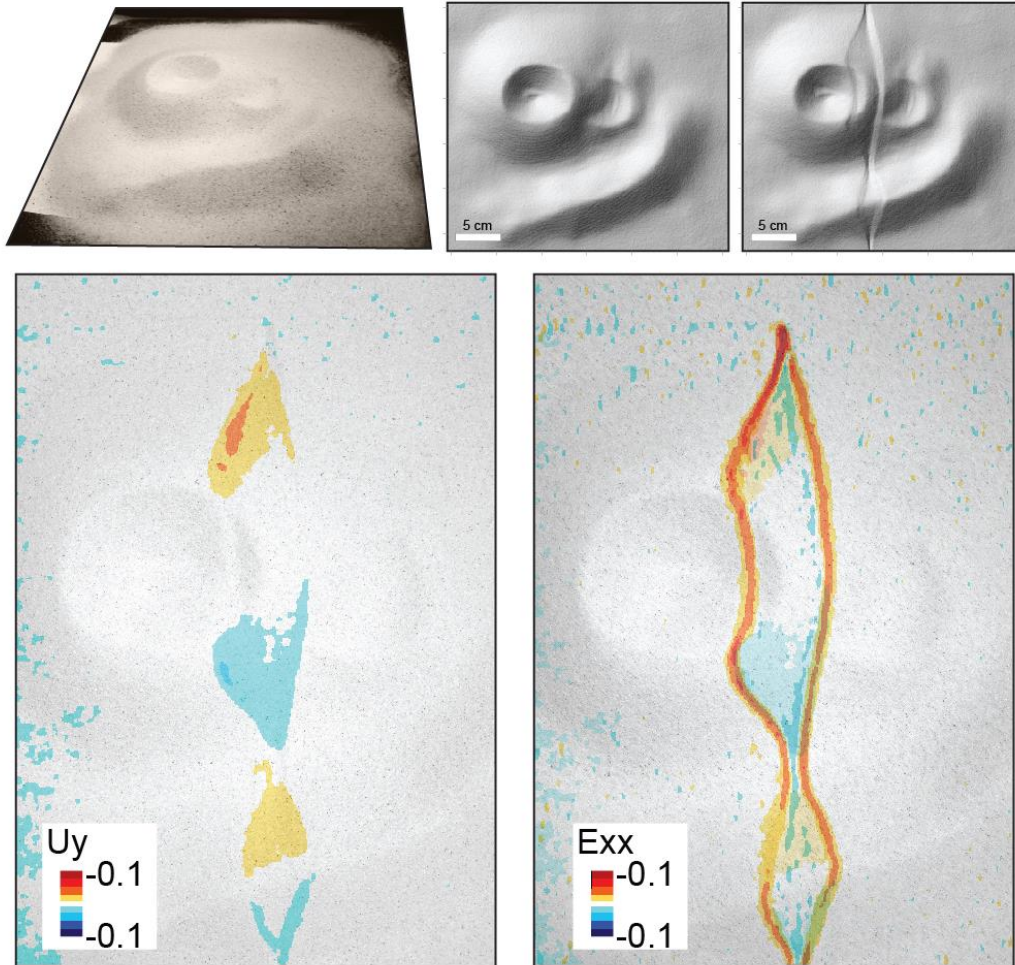


Figure S6

Complex morphology experiment setup and results. Using the same method as described for the single ridge topography experiment, we designed complex morphology experiments. As shown in the perspective photography, these include a ridge on the south side, and two overlapping cones with craters in the centre. This complex topography is manually realised by sieving the setup to the desired dimension. Tensile faulting is realised, affecting the entire complex morphology. Developing graben faults diverge at topographic highs, and converge at topographic lows, with large trend changes at the main cone and crater, mimicking the geometric arrangement identified at the La Palma eruption site. Deformation and strain maps reveal horizontal motion (U_y) and extension (E_{xx}), which is rotated in **Figure 8** to correspond to the orientation of a NE-SW fracture set.